ISSN1027-5495. Functional Materials, 32, No.3 (2025), p. 411-417
doi:http://dx.doi.org/10.15407/fm32.03.411 © 2025 — STC "Institute for Single Crystals"

From microstructure to properties: fractal patterns in carbon steels

D.B. Hlushkova[1], V.M. Volchuk[2], O.V. Orel[1], D.B. Sereda[3]

[1] Kharkiv National Automobile and Highway University, 25 Yaroslava Mudrogo Str., 61002 Kharkiv, Ukraine
[2] Prydniprovska State Academy of Civil Engineering and Architecture, 24a Architect Oleh Petrov Str., 49000 Dnipro, Ukraine
[3] Kremenchuk Mykhailo Ostrohradskyi National University 20 University Str., 39600 Kremenchuk, Ukraine

Received May 25, 2025

Using multifractal analysis, the microstructural homogeneity in carbon alloys after different heat treatment regimes was quantitatively assessed. The sizes of the regions within which the fractal dimension of individual structural elements does not change are established: for lamellar pearlite – 5.3×5.3 μm, for pearlite and residual austenite – 6.2×6.2 μm, for martensite – 4.4×4.4 μm. The homogeneity is expressed through the fractal dimension of each structural component and hardness (HRC). Comparison of the results obtained by traditional metallography and multifractal analysis methods confirmed the complementarity of the approaches and showed the high sensitivity of multifractal analysis to structural changes in the material. The use of digital methods of multifractal analysis opens up prospects for optimizing heat treatment modes and predicting the mechanical properties of carbon alloys.
Keywords: carbon steels, multifractal, structure, hardness, fractal dimensions, forecast.

Від мікроструктури до властивостей: фрактальні закономірності у вуглецевих сталях. *Д.Б. Глушкова, В.М. Волчук, О.В. Орел, Д.Б. Середа*

За допомогою мультифрактального аналізу кількісно оцінили мікроструктурну однорідність у вуглецевих сплавах після різних режимів термічної обробки. Авторами встановлені розміри областей, в межах яких фрактальна розмірність для конкретних елементів структур не змінюється: 5.3×5.3 мкм для пластинчастого перліту, 6.2×6.2 мкм для перліту та залишкового аустеніту, 4.4×4.4 мкм для мартенситу. Однорідність виражається через фрактальну розмірність кожного структурного компонента, і твердість (HRC). Порівняння результатів, отриманих методами традиційної металографії та мультифрактального аналізу, підтвердило взаємодоповнюваність підходів і показало високу чутливість мультифрактального аналізу до структурних змін матеріалу. Використання цифрових методів мультифрактального аналізу відкриває перспективи оптимізації режимів термічної обробки та прогнозування механічних властивостей вуглецевих сплавів.

1. Introduction

Structural heterogeneity of metals and alloys significantly affects their physical and mechanical properties, determining the quality of rolled metal and the residual resource of metal structures [1-4]. Traditional heat treatment methods, such as annealing and hardening, allow for partial elimination of heterogeneity, but operational factors (high temperatures, aggressive environments, dynamic loads) contribute to its re-occurrence. To assess heterogeneity in production conditions, standard scales are used, based on visual analysis of the grain structure, carbide distribution and striations. However,

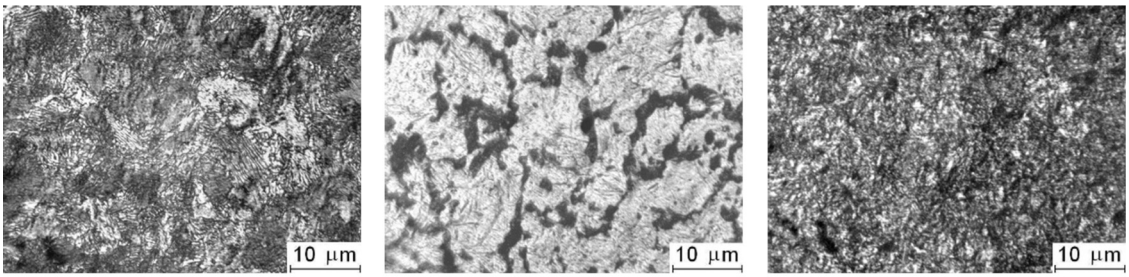

a *b* *c*

Fig. 1. Structure of U8 steel: *a* – lamellar pearlite (sample 1); *b* – pearlite separated along the boundaries of former austenite grains + martensite (sample 2); *c* – martensite (sample 3).

these methods are limited to qualitative assessment and do not always take into account the quantitative characteristics of non-equiaxial particles and their spatial distribution, which requires the development of new approaches [5-8]. At the nano level, the structure is also heterogeneous [9, 10]. To describe the structure, properties and technological processes, mathematical analysis methods [11], digital neural networks [12], synergistic approach [13] and other advanced methods are used.

In this paper, a method using fractal theory [14, 15] and multifractal analysis [16] is proposed for quantitative assessment of microstructural heterogeneity of steels. In contrast to traditional approaches based on qualitative characterization, the method analyzes the distribution of pixels in digital images of the microstructure in two-dimensional space [17]. This makes it possible to identify the relationship between microstructural components and physical and mechanical properties of the material. The results obtained prove the effectiveness of multifractal analysis for improving the quality and predicting the durability of metal products, opening up prospects for express quality control of materials.

2. Material and methods

The material chosen for the study was carbon steel U8, which is widely used for the production of general-purpose tools. The relevance of choosing U8 steel is that during operation, products made of it (cutters, saws, rolled rollers, chisels, etc.) are subject to dynamic loads causing the development of structural heterogeneity, which affects operational properties [18]. For the study, samples of U8 steel without heat treatment were taken, the chemical composition (% by mass) of which is given in Table 1.

The samples were made with a length of 40 mm and a cross section of 5×5 mm. Table 2 shows their heat treatment modes and hardness. Three heat treatment modes were chosen for the research. The holding time for heating in the oven was chosen to be 30 minutes for all samples. To increase the reliability of the results, three hardness measurements were carried out in different zones of the sample from the center to the edge of the sample.

Metallographic studies were performed using a Neophot 2 light microscope (Carl Zeiss) at a magnification of ×1000. To reveal the microstructure, sections of U8 steel samples were etched in a 4% solution of nitric acid in ethyl alcohol. The microstructure in the central zone of the samples is shown in Figure 1.

To quantitatively assess the homogeneity of structural elements (pearlite, austenite, martensite), multifractal analysis was used, based on the processing of digital images of the microstructure [19-21]. This makes it possible to analyze the spatial distribution of local defects of structural elements in the two-dimensional space of the sample, expressed in dimensional characteristics.

The multifractal analysis algorithm included the following steps:

1. Image digitization: The microstructure was recorded with an Olympus C-50 digital camera with a resolution of 510×680 pixels in 256-color*.bmp format (grayscale).

Table 1. Chemical composition of U8 steel

C	Si	Cu	Mn	Ni	P	Cr	S
0.81%	0.17%	0.25%	0.17%	0.25%	0.30%	0.20%	0.03%

Table 2. Heat treatment regimes and hardness of U8 steel

Sample No.	Heat treatment mode	Hardness distribution (HRC) from the center of the sample *r*						
		land (-20 mm)	Thickness 1/2 (-10 mm)	Thickness 1/4 (-5 mm)	center (0 cm)	Thickness 1/4 (5 mm)	Thickness 1/2 (10 mm)	land (20 mm)
1	780 ^{0} C, cooling in the furnace (annealing)	40	39	37	36	37	38	39
2	780 ^{0} C, oil quenching	69	68	67	65	66	68	68
3	780 ^{0} C, water quenching	75	74	73	71	72	73	75

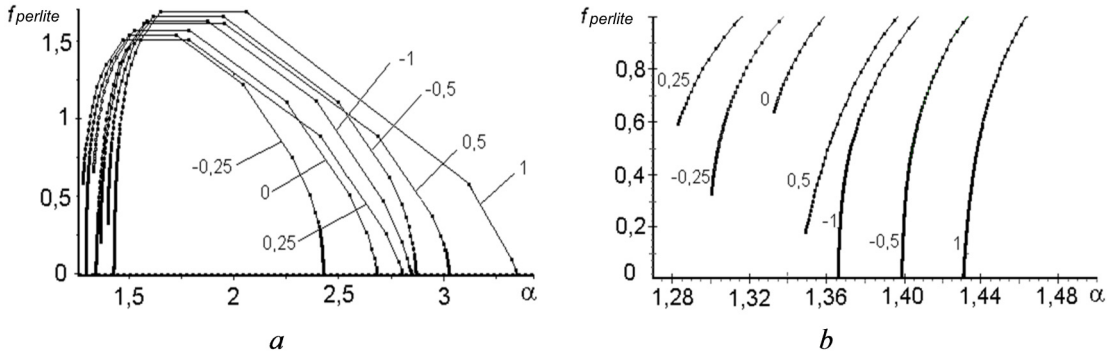

Fig. 2. Multifractal dimension spectra calculated for pearlite (sample 1) at different distances *r* (cm) from the center of the sample (*a*) and an enlarged fragment of the left part of the spectrum (*b*).

2. Discrete approximation: the microstructure was divided into square cells $\varepsilon_к \times \varepsilon_k$ pixels, where ε_k ranged from 20 to 100 pixels (k = 1, 2, ..., 17) with a step of 5 pixels, which corresponds to the physical dimensions of the structural elements from 3.53×3.53 μm to 17.65×17.65 μm. The probability of filling the cells n and the generalized statistical sum is $Z(q,\varepsilon)=\sum_{i=1}^{N} p_i^q \propto \varepsilon^{-\tau(q)}$, where q is a power index in the range from (-300) to (+300), normalized by the formula $\sum_i p_i = 1$.

3. The mass index $\tau(q)=\lim_{\varepsilon\to 0}\frac{\ln Z(q)}{\ln \varepsilon}$ was defined as a measure of the density of cells filled with pixels, reflecting the probability of the distribution of structural elements. The index characterizes the areas with the highest density $q=-300.$, with the lowest density $q=+300$.

4. The canonical spectrum of singularities $f(\alpha)$ was calculated using the Legendre transformation $\tau(q)$: $f(\alpha)=q\alpha-\tau(q)$, where the Hölder index α s defined as $\alpha=\frac{d\tau(q)}{dq}$. The spectrum represents the Hausdorff dimensions of the microstructure subsets that contribute most to the statistical sum *q*.

The homogeneity of the microstructure was assessed by the deviation of the right and left parts of the spectrum from zero (see Fig. 2 and 3). A detailed analysis is presented in the section "Results and Discussion".

3. Results and discussion

Multifractal analysis allowed us to determine the maximum sizes of the microstructure regions where the homogeneity of structural elements is maintained for three heat treatment modes of U8 steel. For sample 1 (annealing, lamellar pearlite, Fig. 1), the grid size was 30×30 pixels (5.3×5.3 μm). For sample 2 (oil quenching, pearlite and retained austenite, Fig. 2), the square grid of the coating was 35×35 pixels (6.2×6.2 μm). For sample 3 (water quenching, martensite, Fig. 3): 25×25 pixels (4.4×4.4 μm). These are the sizes of the areas in which the structural elements maintain their uniform distribution.

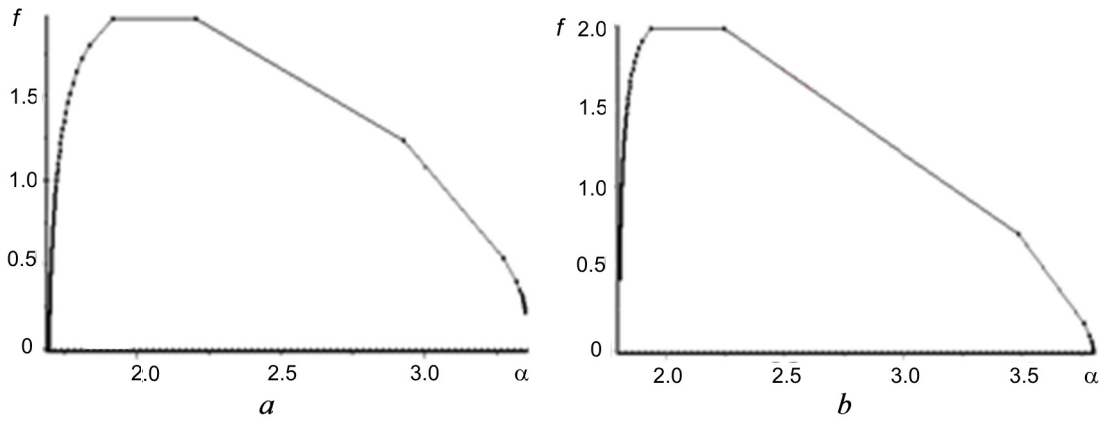

Fig. 3. Singularity spectrum calculated for retained austenite at a distance r = 20 mm from the center of sample 2 (oil quenching) (*a*) and martensite at a distance r = 10 mm from the center of sample 3 (*b*) (water quenching).

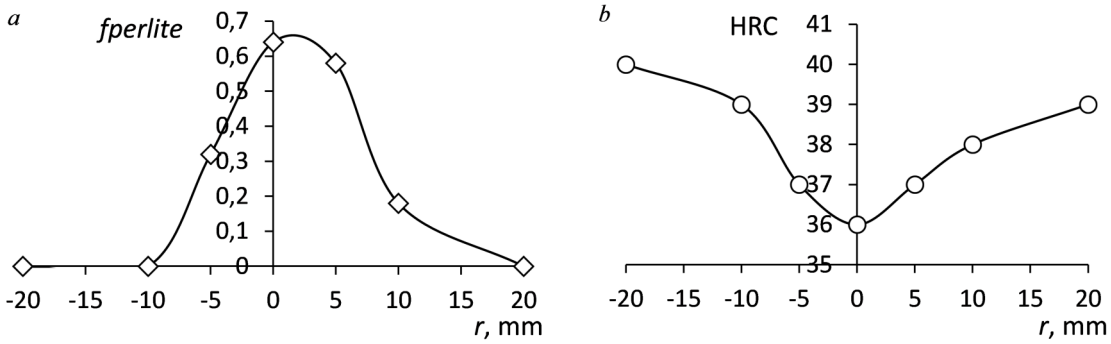

Fig. 4. Change in the homogeneity of lamellar pearlite depending on the distance along the cross-section of sample 1 (a); hardness distribution along the cross-section of sample 1 (b).

The fractal dimension distribution spectra calculated for different structural components are shown in Figures 2 and 3. For lamellar perlite (sample 1), the spectra are calculated at different distances from the center of the sample: r = 0.5, 1, 2 cm). Figure 2a shows the fractal dimension distribution spectra of perlite, and Figure 2b shows an enlarged fragment of the left part of the spectra, which is used to assess uniformity. The uniformity values for perlite were: 0.64 for r = 0; 0.58 and 0.32 for r = ±0.5; 0.18 for r = 1 and 0 for r = 1, -2 and 2.

The deviation of the left part of the spectrum $f(\alpha)$. from zero characterizes the homogeneity of the close-packed regions of the microstructure corresponding to dark elements (e.g., pearlite in sample 1, martensite in sample 3). For martensite (sample 3), the homogeneity was f = 0.44 (Figure 3b). In contrast, the deviation in the right part of the spectrum indicates the homogeneity of regions containing light elements, such as retained austenite in sample 2 (f = 0.22) (Figure 3a).

To assess the practical significance of the results of the multifractal analysis, they were compared with data obtained by traditional methods of quantitative metallography. The microstructure of sample 1 (annealing, 780 °C, furnace cooling, Fig. 1a) is characterized by high uniformity over the entire cross section and consists mainly of lamellar pearlite (dark areas) with a small proportion of peritectoid ferrite 2-3% (light areas), as shown in Fig. 1a. Such a structure is formed as a result of the diffusion redistribution of carbon from austenite to cementite during pearlitic transformation due to slow cooling. The dimensions of lamellar pearlite correspond to 4 points.

Quantification of the homogeneity of lamellar pearlite, performed using multifractal analysis, revealed its structural sensitivity. The homogeneity value varied across the entire cross-section of the sample (Figure 4a) in correlation with the hardness (Figure 4b).

The decrease in the homogeneity of lamellar pearlite from the center to the edge of sample 1 (Figure 4a) is associated with an increase in local defects, which is confirmed by a decrease in the fractal dimension of pearlite from 1.55 in the center to 1.51 at the edges. This correlates

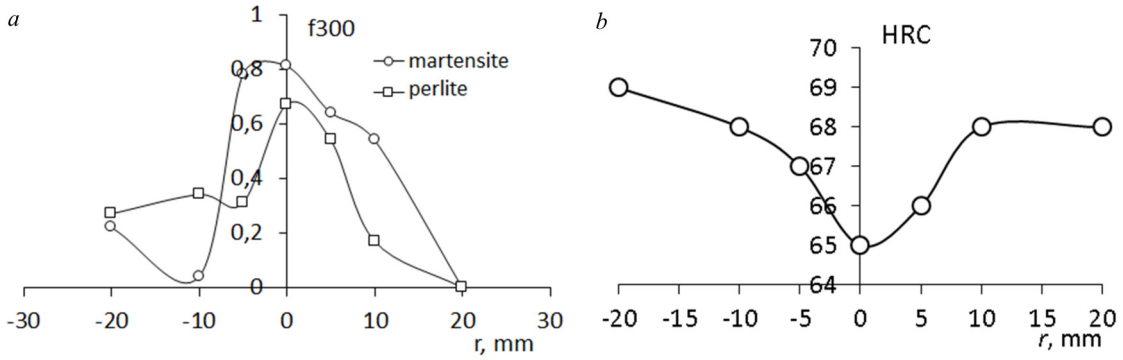

Fig. 5. Dependence of the homogeneity of martensite of sample 2 on the distance to the center (a) and the hardness distribution over the cross section of sample 2 (b).

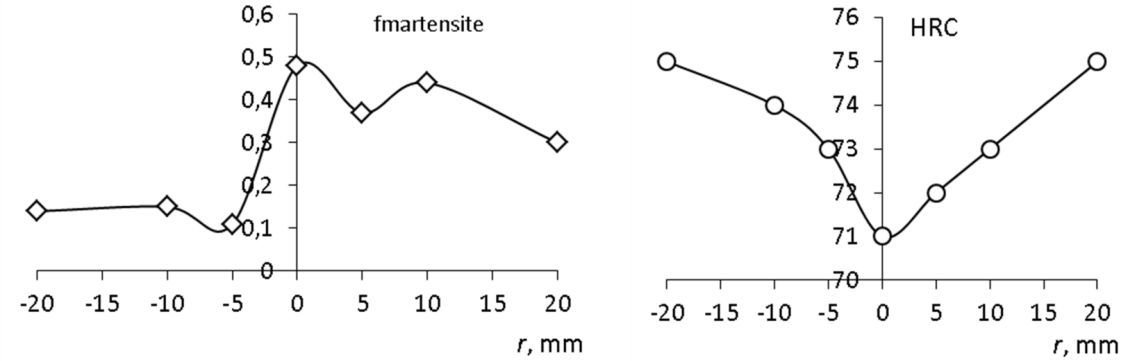

Fig. 6. Dependence of the homogeneity of martensite of sample 3 on the distance to the center (a) and the hardness distribution over the area of sample 3 (b).

with a change in hardness (Figure 4b), which increases from 36 HRC in the center to 40 HRC at the edge. The obtained data indicate that hardness as a local characteristic of the microvolume of a carbon alloy depends on the spatial defect of the microstructure, expressed in the dimensional units of multifractal analysis.

The microstructure of sample 2 (oil quenching, Figure 1b) consists of pearlite, which is isolated along the boundaries of the former austenite grains (dark areas), as well as martensite (light areas). The homogeneity of such a structure is due to the semi-diffusion transformation of austenite with a partial martensite transformation, which is accompanied by diffusional redistribution of carbon. Differences in the cooling rate across the entire cross-section of the sample contributed to a change in the phase composition: the proportion of pearlite decreased from 16% in the center to 7% at the edge, and the proportion of martensite increased.

The microstructure of sample 3 (water quenching, Fig. 1c) consists of lamellar martensite (about 92%, dark areas) and retained austenite (about 8%, light areas) throughout the cross section. The homogeneity of the microstructure, determined by multifractal analysis at a magnification of ×1000, reflects the features of the microrelief of lenticular martensite plates formed as a result of shear transformation of austenite due to cooperative displacement of atoms. This morphology of the plates minimizes the energy of elastic distortions in the austenite matrix.

The decrease in the homogeneity of martensite from the center to the edge of the sample (Figure 6a) may be associated with an increase in local defects at the substructural level, which is associated with the difference in cooling rate. This is confirmed by the decrease in the fractal dimension of martensite from 1.97 in the center to 1.74 at the edge. The substructural changes affecting the defects include an increase in the density of dislocations, an increase in internal stresses of the second kind, and a decrease in the size of subgrains with stable α-Fe lattice parameters. These changes correlate with an increase in hardness from 71 HRC in the center to 75 HRC at the edge (Figure 6b), which indicates an improvement in the strength properties from the center to the surface of the sample.

The obtained results demonstrate the high sensitivity of the hardness of the carbon alloy to the homogeneity characteristics determined by multifractal analysis. In particular, changes in homogeneity due to local defects and phase composition correlate with hardness. This correlation confirms that multifractal analysis is a tool for quantitative assessment of microstructure and property prediction.

4. Conclusion

The paper considers the possibility of using multifractal analysis to quantitatively assess the morphology of structural components of a carbon alloy after various heat treatment regimes. The homogeneity of the structure, expressed through spatial defects of dimensional indices, is determined, and the maximum sizes of regions of uniform distribution of structural elements are established.

Comparison of the homogeneity with hardness indices (HRC) revealed their correlation, caused by changes in local microstructural defects. In all samples, a decrease in homogeneity from the center to the edge was associated with an increase in defects (e.g., dislocation density and internal stresses) due to the difference in cooling rates. For sample 1, the fractal dimension of pearlite decreased from the edge to the center from 1.55 to 1.51; for sample 3, the fractal dimension of martensite decreased from 1.97 at the edge to 1.74 in the center. These results correlated with an increase in hardness from 36 to 40 HRC for sample 1 and from 71 to 75 HRC for sample 3, respectively.

It is shown that multifractal analysis of microstructure, in comparison with traditional methods of quantitative metallography, surpasses them in sensitivity to substructural changes and geometric complexity of the microstructure, which makes it a promising tool for assessing physical and mechanical properties.

References

1. G.I. Zaginaylov, V.I. Shcherbinin, K. Schuenemann, M.K. Thumme, *IEEE Transactions on Plasma Science*, **34**(3), 512 – 517 (2006) https://doi.org/10.1109/TPS.2006.875760
2. Y. Gutarevych, V. Mateichyk, J. Matijošius, A. Rimkus, I. Gritsuk, O. Syrota, Y. Shuba, *Energies*, **13**(5), 1076 (2020) https://doi.org/10.3390/en13051076
3. P. Andrenko, A. Rogovyi, I. Hrechka, S. Khovanskyi, M. Svynarenko, *Journal of Physics: Conference Series*, **1741**(1) (2021) https://doi.org/10.1088/1742-6596/1741/1/012024
4. V. Maslova, R. Nastase, G. Veryasov, N. Nesterenko, E. Fourré, C. Batiot-Dupeyrat, *Progress in Energy and Combustion Science*, **101**, 101096 (2024) https://doi.org/10.1016/j.pecs.2023.101096
5. Vafaeva, K.M., Dhyani, M., Acharya, P., Parik, K., Ledalla, S., *Bio Web of Conferences*, **86**, 01111 (2024) https://doi.org/10.1051/bioconf/20248601111
6. D.B. Hlushkova, O.D. Hrinchenko, L.L. Kostina, A.P. Cholodov, *Problems of Atomic Science and Technology*, **1**(113), 181-188 (2018).
7. Migal V., Lebedev A., Shuliak M., Kalinin E., Arhun S., Korohodskyi V. *Journal of Vibration and Control*, **27**, 1123 – 1131 (2021) https://journals.sagepub.com/doi/10.1177/1077546320937634
8. M. Krbata, M. Kohutiar, J. Escherova et. al. *Applied Mechanics*, **6**(1), 16. (2025). https://doi.org/10.3390/applmech6010016
9. N.E. Kalinina, D.B. Glushkova, A.I. Voronkov, V.T. Kalinin. Functional Materials, 26(3), 514–518 (2019) https://doi.org/10.15407/ fm26.03.514
10. D.B. Hlushkova, A.V. Kalinin, N.E. Kalinina, V.M. Volchuk, V.A. Saenko, A.A. Efimenko, *Problems of Atomic Science and Technology*, **144**(2), 126 (2023) https://doi.org/10.46813/2023-144-126
11. D. Leontiev, O.I. Voronkov, V. Korohodskyi, D. Hlushkova, I. Nikitchenko, E. Teslenko, O. Lykhodii, *SAE Technical Paper*, 2020-01-2222 (2020) https://doi.org/10.4271/2020-01-2222
12. A.I. Borovkov, K.M. Vafaeva, N.I. Vatin, I. Ponyaeva, *Construction Materials and Products*, **7**(4), 7 (2024) https://doi.org/10.58224/2618-7183-2024-7-4-7
13. M. Rajendran, M. Arumugam, L. Sourirajan et. al., *Results in Engineering*, **26**, 104614 (2025) https://doi.org/10.1016/j.rineng.2025.104614
14. Sergiyenko O.,Hernández Balbuena, D., Tyrsa V., Rosas Méndez, Patricia Luz A. Lopez M. R, Hernandez W, Podrygalo M., Gurko A. *Journal of the International Measurement Confederation*, **44**, 1229 – 1242 (2011) https://www.sciencedirect.com/science/article/abs/pii/S0263224111001254?via%3Dihub
15. C. Ding, L. Jiang, J. Xu, S. Guo, J. Zhang, P. Xiong, Z. Piao, *International Journal of Bifurcation and Chaos*, **35**(08), 2550098 (2025) https://doi.org/10.1142/S0218127425500981
16. P. Zhang, J. Ding, J. Guo, F. Wang, *Fractal and Fractional*, **8**(6), 304 (2024) https://doi.org/10.3390/fractalfract8060304
17. K.M. Vafaeva, N.I. Vatin, D.F. Karpov, V. Romanovski, *Materials Research Express*. **12,**

075307 (2025) https://doi.org/10.1088/2053-1591/adf161
18. D.B. Hlushkova, V.M. Volchuk, *Functional Materials*, 30(3), 453 (2023) https://doi.org/10.15407/fm30.03.453
19. D. Kakimzhanov, B. Rakhadilov, L. Sulyubayeva, M. Dautbekov, *Coatings*, **13**(11), 1824 (2023).
20. D.B. Hlushkova, V.M. Volchuk, P.M. Polyansky, V.A. Saenko, A.A. Efimenko, *Functional Materials*, **30**(2) 275 (2023) https://doi.org/10.15407/fm30.02.275
21. Y. Wang, A. Karasev, J.H. Park, P.G. Jönsson, *Metall Mater Trans*, B **52**, 2892–2925 (2021). https://doi.org/10.1007/s11663-021-02259-7